# Dependency of Phosphorescence Energy Transfer Rate on Distance between a Cationic Donor and a Cationic Acceptor and on Temperature

**Akio Yoshimura,* Koichi Nozaki, Noriaki Ikeda, and Takeshi Ohno***

Department of Chemistry, Graduate School of Science, Osaka University, 1-16 Machikaneyama, Toyonaka, Osaka 560

(Received April 22, 1996)

Phosphorescence energy transfer within ligand bridged diruthenium(II) compounds of the form $[(bpy)_2Ru(II)(B)Ru(II)(becbpy)_2]^{4+}$, where bpy, becbpy, and B are 2,2′-bipyridine, 4,4′-bis(ethoxycarbonyl)-2,2′-bipyridine, and a bridging ligand, respectively, was investigated in butyronitrile solution in the temperature range 77—330 K. Excitation energy transfer occurs from the $Ru(bpy)_2^{2+}$ moiety to the $Ru(becbpy)_2^{2+}$ moiety. The energy transfer rate ($k_{EN}$=(0.4—7.4)$\times 10^6$ $s^{-1}$) at 77 K is weakly dependent on the $Ru^{2+}$–$Ru^{2+}$ distance ($r$), which is estimated for the extended conformer of the bridging ligand. A linear plot of $\log k_{EN}$ vs. $\log(1/r^6)$ shows that energy transfer occurs via the dipole–dipole interaction. The weak temperature-dependence of the energy transfer rate in the temperature range 77—110 K is explained in terms of the absorption–emission coupling integral. The fast energy transfer ($55\times 10^6$ $s^{-1}$) within $[(bpy)_2Ru(bpbimH_2)Ru(becbpy)_2]^{4+}$ (bpbimH$_2$=2,2′-di-(2-pyridyl)-6,6′-bibenzimidazole) at 77 K is ascribed to the substantial exchange interaction between the $Ru(bpy)_2(bpbimH_2)^{2+}$ moiety in the excited state and the $Ru(becbpy)_2^{2+}$ moiety in the ground state.

Electron transfer reactions in covalently linked donor–acceptor compounds have been investigated over the past decade by means of laser flash photolysis spectroscopy. The dependence of the rate of the reactions on the energy gap,[1—3] temperature,[4—7] solvent relaxation time,[6,8—10] and donor–acceptor distance[11—14] has been examined for many donor–acceptor molecules. The rates of nonadiabatic electron transfer ($k_{ET}$) can be estimated by using a Franck–Condon weighted density (FCWD), assuming a common vibrational frequency ($\nu_n$) for both the reactants and the products (Eq. 1).[15]

$$k_{ET} = \frac{(2\pi)^2 H_{rp}{}^2}{h\sqrt{4\pi\lambda_o k_B T}} \sum_m \frac{S^m e^{-S}}{m!} \exp\left(-\frac{(\Delta E^\circ - \lambda_o - mh\nu_n)^2}{4\lambda_o k_B T}\right). \quad (1)$$

Here, $H_{rp}$, $\Delta E^\circ$, $\lambda_o$, $S$, and $m$ are the matrix element between the reactants and products, the energy gap of energy transfer reaction, the reorganization energy of low-frequency solvent mode, the Huang–Rhys factor, and the quantum number of the high-frequency vibrational mode involved in the electron transfer, respectively.

Equation 1 can also be applied to an estimation of the rate of phosphorescence energy transfer by using $\lambda_o$, $S$, and $\nu_n$; the FCWD of the emission and absorption processes can be evaluated. Therefore, the FCWD of energy transfer can be expressed in terms of the normalized emission intensity of the donor ($f_D(\tilde{\nu})$) and the normalized absorption intensity of the acceptor ($f_A(\tilde{\nu})$) instead of $S$ and $\lambda_o$ (Eq. 2).[16,17]

$$k_{EN} = \frac{(2\pi)^2 H_{rp}^2}{h^2 c} \int_0^\infty f_D(\tilde{\nu}) f_A(\tilde{\nu}) d\tilde{\nu}. \quad (2)$$

Hereafter, the integral of Eq. 2 will be called the absorption–emission overlap.

When the matrix element of energy transfer arises from dipole–dipole interactions, the magnitude of the rate can be expressed by Eq. 3 by using the distance between the transition dipoles ($r$), the natural lifetime of the donor ($\tau_o$), $f_D(\tilde{\nu})$, the molar absorption coefficient of the acceptor ($\varepsilon_A(\tilde{\nu})$), and the refractive index of the solvent ($n$).[18] The FCWD is mixed with the transition dipoles of absorption and emission in Eq. 3, the integral of which denotes the absorption–emission coupling.

$$k_{EN} = \frac{9000 \ln 10}{128\pi^5 n^4 N_o r^6 \tau_o} \int_0^\infty \frac{f_D(\tilde{\nu}) \varepsilon_A(\tilde{\nu})}{\tilde{\nu}^4} d\tilde{\nu}. \quad (3)$$

A few studies have been done on the rate of excitation energy transfer of metal-to-ligand charge transfer (MLCT) states. Most recently, a small reorganization energy of a low-frequency vibrational mode and a high-frequency mode were obtained by means of simulation from the rate of energy-gap dependent energy transfer, MLCT⟹π–π*, at 300 K.[19,20] The temperature dependence of the energy-transfer rate suggested a small reorganization energy for MLCT⟹d–d* energy transfer.[21]

The nonadiabaticity of excitation energy transfer has been explained in terms of the rapidly decreasing magnitude of two-center two-electron exchange integral with increase in donor–acceptor distance.[22—25] Dipole–dipole interactions between a donor and an acceptor can be responsible for the energy transfer because of the gradual decrease of the interaction strength with an increase in distance in a relative sense. It has been proposed that the dipole–dipole interaction is predominant for slow excitation energy transfer within donor–acceptor compounds containing a heavy metal ion such as Ru(II)[26,27] and Os(II).[28] The excitation of solvent phonons[21] and the low- and high-frequency vibrations of the products[19,20] have been suggested by the non-bell-shaped

dependence of the phosphorescence energy transfer rate on the energy gap. Fast energy transfers have been observed for covalently linked donor–acceptor composite molecules.[29—32]

In this paper we describe the distance- and temperature-dependencies of the charge-transfer excitation energy transfer within ligand bridged compounds of the form of $[(bpy)_2Ru(B)Ru(becbpy)_2]^{4+}$, where bpy, becbpy, and B are 2,2′-bipyridine, 4,4′-bis(ethoxycarbonyl)-2,2′-bipyridine, and a bridging ligand, respectively. As the structures of the compounds in Fig. 1 show, the distances between the cationic chromophores of $Ru(bpy)_2^{2+}$ and $Ru(becbpy)_2^{2+}$ are dependent on the kind of the bridging ligand. The observed rates of the energy transfer processes at 77 K are compared with those calculated by assuming dipole–dipole interactions. The temperature-dependence of the energy transfer rate is compared with that of either the absorption–emission coupling integral or the FCWD in a temperature region 77—330 K. The rate of the energy transfer within the ligand bridged compounds of the form $[(bpy)_2Ru(B)Ru(becbpy)_2]^{4+}$ will be compared with the rate of electron transfer within the ligand bridged compounds of the form $[(bpy)_2Ru(B)Ru(becbpy)_2]^{5+}$.[33]

## Experimental

**Materials.** Butyronitrile was purified by distillation over $P_2O_5$ under a reduced pressure.

**Preparation. The Bridging Ligands:** All the bridging ligands (B) contain two chelating 2-(2-pyridyl)-1-benzimidazolyl groups (L). Bridging ligands of 1,3-bis[2-(2-pyridyl)-1-benzimidazoyl]propane (L–$(CH_2)_3$–L), 1,4-bis[2-(2-pyridyl)-1-benzimidazolyl]butane (L–$(CH_2)_4$–L), 1,5-bis[2-(2-pyridyl)benzimidazolyl]-pentane (L–$(CH_2)_5$–L), 1,6-bis[2-(2-pyridyl)-1-benzimidazolyl]-hexane (L–$(CH_2)_6$–L), 1,10-bis[2-(2-pyridyl)-1-benzimidazolyl]-decane (L–$(CH_2)_{10}$–L), and *p*-bis[[2-(2-pyridyl)-1-benzimidazolyl]-methyl]benzene (L–Xy–L) were synthesized by the coupling 2-(2-pyridyl)benzimidazole (pbimH) with $\alpha,\omega$-dibromoalkane or *p*-bis(bromomethyl)benzene in dry *N*,*N*-dimethylformamide in the following manner. Sodium hydride (0.25 g) was added under an argon atmosphere to a solution of well-dried pbimH (1 g) in dried *N*,*N*-dimethylformamide (15 ml). The mixture was heated for 1 h. After addition of dibromoalkane (0.5 g), the solution was refluxed for 2 h. During refluxing, NaBr precipitated and the solution turned dark brown. After the addition of water (30 ml) to the solution, the product was extracted with chloroform (120 ml). Evaporation of the chloroform gave the crude product, which was loaded onto

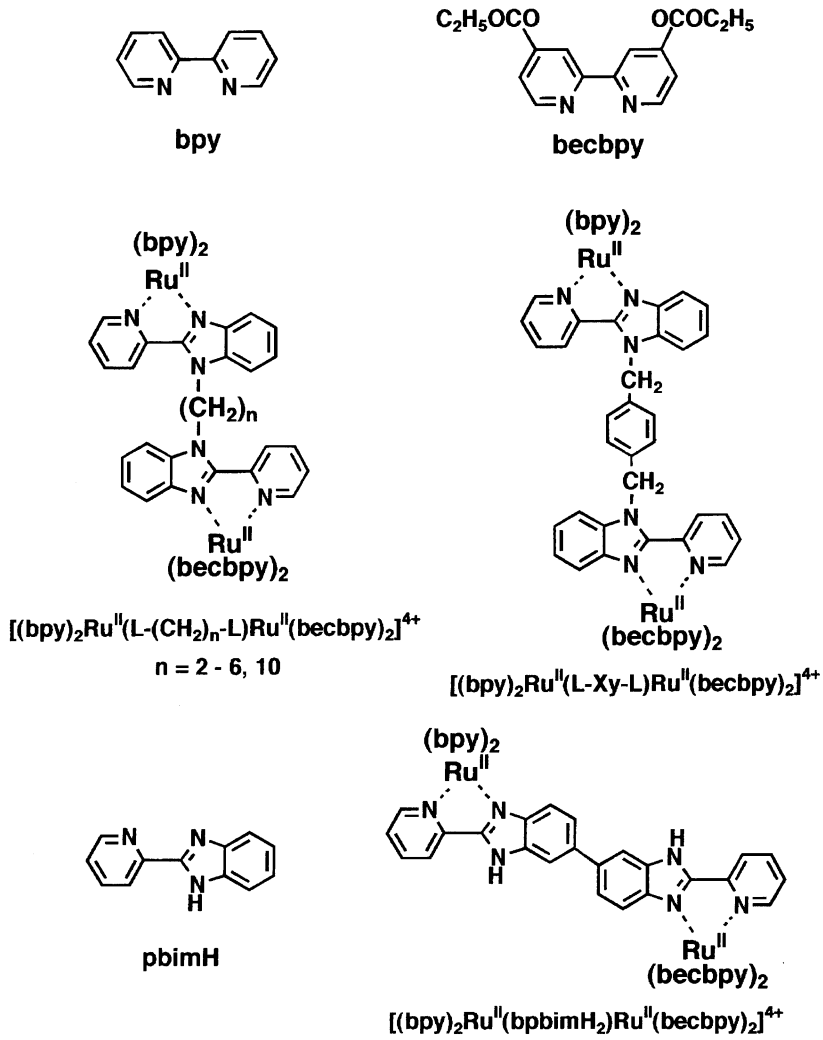


Fig. 1. Component molecules and abbreviations.

an alumina column and eluted with toluene–dichloromethane. The compound obtained from the third band was recrystallized twice from a mixture of chloroform and ethyl acetate.

**The Mononuclear complex of $[Ru(L')_2(L\text{–}(CH_2)_n\text{–}L)](ClO_4)_2$ and $[Ru(L')_2(L\text{–}Xy\text{–}L)](ClO_4)_2$ (L'=bpy or becbpy, $n$=2—6, 10):** A mixture of $[Ru(L')_2Cl_2]$ (60 mg) and an equimolar amount of a bridging ligand in ethanol/water (1 : 1 v/v) was refluxed for 4 h. The product was purified on an SP-Sephadex cation-exchange column using a mixture (1 : 1 v/v) of acetonitrile and an aqueous Britton–Robinson buffer (pH 4.6).[34] The preparation method of $[Ru(bpy)_2(L\text{–}(CH_2)_2\text{–}L)](ClO_4)_2$ has been described previously.[35,36] The complex was recrystallized from ethanol/water. Yield 150—170 mg.

**$[Ru(bpy)_2(L\text{–}(CH_2)_5\text{–}L)](ClO_4)_2\cdot H_2O$:** Found: C, 54.26; H, 4.10; N, 12.84%. Calcd for $C_{49}H_{42}Cl_2N_{10}O_8Ru\cdot H_2O$: C, 54.05; H, 4.07; N, 12.86%.

**$[Ru(becbpy)_2(L\text{–}(CH_2)_5\text{–}L)](ClO_4)_2\cdot 4H_2O$:** Found: C, 51.22; H, 4.40; N, 9.83%. Calcd for $C_{61}H_{58}Cl_2N_{10}O_{16}Ru\cdot 4H_2O$: C, 51.19; H, 4.65; N, 9.79%.

**The Diruthenium Complexes of $[Ru(bpy)_2(L\text{–}(CH_2)_n\text{–}L)Ru(becbpy)_2](PF_6)_4$ and $[Ru(bpy)_2(L\text{–}Xy\text{–}L)Ru(becbpy)_2](PF_6)_4$:** A mixture of $[Ru(becbpy)_2Cl_2]$ (20 mg) and $[Ru(bpy)_2(L\text{–}(CH_2)_n\text{–}L)](ClO_4)_2$ or $[Ru(bpy)_2(L\text{–}Xy\text{–}L)](ClO_4)_2$ (25 mg) in 10 mL of ethanol/water (1 : 1 v/v) was refluxed for 7 h. The product was purified on a CM-Sephadex cation-exchange column using a mixture of acetonitrile and the Britton–Robinson buffer solution of pH 5.7 (1 : 1 v/v) containing 50 mM $NH_4PF_6$. The complex was recrystallized from ethanol/water. Yield 10—20 mg.

**$[Ru(bpy)_2(L\text{–}(CH_2)_2\text{–}L)Ru(becbpy)_2](PF_6)_4\cdot 2H_2O$:** Found: C, 43.52; H, 3.48; N, 9.10%. Calcd for $C_{78}H_{68}F_{24}N_{14}O_8P_4Ru_2\cdot 2H_2O$: C, 44.63; H, 3.38; N, 9.13%.

**$[Ru(bpy)_2(L\text{–}(CH_2)_3\text{–}L)Ru(becbpy)_2](PF_6)_4$:** Found: C, 44.22; H, 3.42; N, 9.31%. Calcd for $C_{79}H_{70}F_{24}N_{14}O_8P_4Ru_2$: C, 44.64; H, 3.32; N, 9.23%.

**$[Ru(bpy)_2(L\text{–}(CH_2)_4\text{–}L)Ru(becbpy)_2](PF_6)_4\cdot 2H_2O$:** Found: C, 44.16; H, 3.38; N, 9.04%. Calcd for $C_{80}H_{72}F_{24}N_{14}O_8P_4Ru_2\cdot 2H_2O$: C, 44.17; H, 3.52; N, 9.01%.

**$[Ru(bpy)_2(L\text{–}(CH_2)_5\text{–}L)Ru(becbpy)_2](PF_6)_4\cdot 2H_2O$:** Found: C, 44.64; H, 3.61; N, 8.99%. Calcd for $C_{81}H_{74}F_{24}N_{14}O_8P_4Ru_2\cdot 2H_2O$: C, 44.43; H, 3.59; N, 8.96%.

**$[Ru(bpy)_2(L\text{–}(CH_2)_6\text{–}L)Ru(becbpy)_2](PF_6)_4$:** Found: C, 45.14; H, 3.62; N, 9.20%. Calcd for $C_{82}H_{76}F_{24}N_{14}O_8P_4Ru_2$: C, 45.44; H, 3.53; N, 9.05%.

**$[Ru(bpy)_2(L\text{–}Xy\text{–}L)Ru(becbpy)_2](PF_6)_4\cdot 2H_2O$:** Found: C, 45.39; H, 3.51; N, 8.77%. Calcd for $C_{84}H_{72}F_{24}N_{14}O_8P_4Ru_2\cdot 2H_2O$: C, 45.37; H, 3.45; N, 8.82%.

**$[Ru(bpy)_2(L\text{–}(CH_2)_{10}\text{–}L)Ru(becbpy)_2](PF_6)_4$:** Found: C, 46.51; H, 3.76; N, 9.08%. Calcd for $C_{86}H_{84}F_{24}N_{14}O_8P_4Ru_2$: C, 46.45; H, 3.81; N, 8.82%.

**The Diruthenium Complex of $[Ru(bpy)_2(bpbimH_2)Ru(becbpy)_2](PF_6)_4$:** A mixture of $[Ru(becbpy)_2Cl_2]$ (20 mg) and $[Ru(bpy)_2(bpbimH_2)](ClO_4)_2$ (25 mg) in 10 mL of ethanol/water (1 : 1 v/v) was refluxed for 4 h. The product, $[Ru(bpy)_2(bpbimH_2)Ru(becbpy)_2](ClO_4)_4$ was purified on an SP-Sephadex cation-exchange column using a mixture of acetonitrile and the Britton–Robinson buffer (pH 4.6) (1 : 1 v/v).

**$[Ru(bpy)_2(bpbimH_2)Ru(becbpy)_2](ClO_4)_4\cdot 6H_2O$:** Found: C, 45.30; H, 3.52; N, 9.51%. Calcd for $C_{76}H_{64}N_{14}O_{24}Cl_4Ru_2\cdot 6H_2O$: C, 45.43; H, 3.81; N, 9.76%.

**Apparatus.** A Hitachi 323 absorption spectrophotometer and a Hitachi MPF-4 spectrofluorometer were used to record the absorption and emission spectra of the Ru(II) compounds, respectively. The sensitivity of the emission measurement was improved through the use of a Usio JPD100V500WCS bromine lamp. The third-harmonic (355 nm, pulse-width 8 ns, 1—10 mJ, 10 Hz) of a nanosecond Nd–YAG laser, (Quantel YG580), and a picosecond Nd–YAG laser, (Continuum PY61C-10; 10Hz, fwhm; 17 ps) were used for the excitation of the Ru(II) compounds.

The decay and the time-resolved spectra of emission were detected by using a Hamamatsu Photonics R3896 photomultiplier. An avalanche PIN photodiode (Hamamatsu Photonics S2383) was used to detect emission with a lifetime shorter than 40 ns. The photocurrent of the photodiode was amplified by the use of a wide-bandwidth preamplifier (Comlinear, CLC 140, 500MHz) and fed into a digitizing oscilloscope (Hewlett-Packard Co., HP54510A, 8 bit, 250 MHz). The time resolution was 0.6 ns. The temperature of the samples in the Oxford DN1704 cryostat was controlled in a range of 77—300 K by the use of an Oxford ITC4 controller. A circulated water bath was used to keep the samples at 300—337 K.

**Procedure.** The butyronitrile solutions of the Ru(II) complexes were deaerated by the bubbling of Ar. In the case of complexes containing $bpbimH_2$ as a bridging ligand, 2 mM $HClO_4$ was added to avoid deprotonation.

## Results

**1. Absorption and Emission Spectra.** The absorption spectrum of $[Ru(becbpy)_2(L\text{–}(CH_2)_5\text{–}L)]^{2+}$ in the region of $(15.4\text{—}25)\times 10^3$ $cm^{-1}$ is not different from that of $[Ru(becbpy)_2(bpy)]^{2+}$.[37] The lowest and weak band in the region of $(15.6\text{—}19)\times 10^3$ $cm^{-1}$ is distinguished from a couple of strong bands above $19\times 10^3$ $cm^{-1}$ by means of multi-Gaussian analysis, as Fig. 2 shows. The intensive band around $20\times 10^3$ $cm^{-1}$ loses its structure at 300 K, while the large full width at half maximum (fwhm) of the broad bands in the lower energy region are nearly independent of temperature. The lowest and weak absorption is assigned to the transition to the triplet charge transfer excited state,

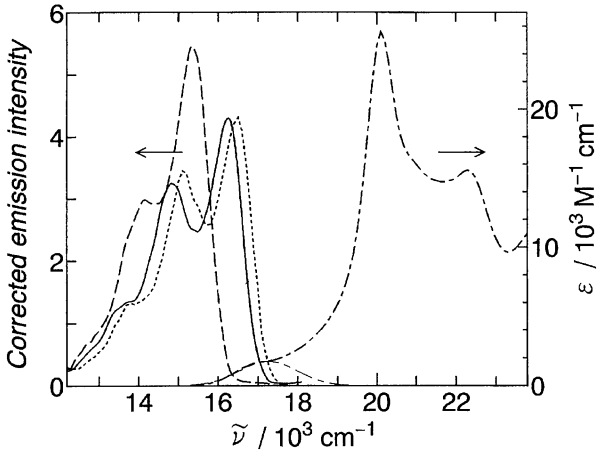


Fig. 2. Emission spectra of $[Ru(bpy)_2(bpbimH_2)Ru(bpy)_2]^{4+}$ (solid line), $[Ru(bpy)_2(L\text{–}(CH_2)_5\text{–}L)]^{2+}$ (dotted line), and $[Ru(bpy)_2(bpbimH_2)Ru(becbpy)_2]^{4+}$ (broken line) and absorption spectrum of $[Ru(becbpy)_2(L\text{–}(CH_2)_5\text{–}L)]^{2+}$ (chain line), with the excitation at 450 nm in butyronitrile at 77 K. A thin chain line shows the singlet–triplet absorption obtained by means of multi-Gaussian analysis of the absorption spectrum.

though the singlet character of the higher states is mixed into the lowest excited state. No new band appeared even for the diruthenium(II) compound with the shortest bridging ligand, $[Ru(bpy)_2(L\text{–}(CH_2)_2\text{–}L)Ru(becbpy)_2]^{4+}$, implying a very weak interaction between the Ru(II) centers. Coordination of $[Ru(bpy)_2(L\text{–}(CH_2)_2\text{–}L)]^{2+}$ to another $Ru(bpy)_2^{2+}$ moiety brings about no shift of the MLCT band, showing that only a very weak interaction exists between the Ru(II) centers.

The emission spectra of the mononuclear and dinuclear Ru(II) compounds consist of three vibronic bands (Table 1). The fwhm of the first emission band is estimated to be 830 $cm^{-1}$ at 77 K as $2\times\Delta\tilde{\nu}_{1/2}$ (see Table 2), where $\Delta\tilde{\nu}_{1/2}$ is the half width at half-maximum on the higher energy side. The energy of the first emission band ($\tilde{\nu}_0$) of the $Ru(bpy)_2(L\text{–}(CH_2)_n\text{–}L)^{2+}$ moiety at 77 K is almost constant ($16.5\times10^3$ $cm^{-1}$), irrespective of the polymethylene chain length. Coordination of the bridging ligand to another $Ru(bpy)_2^{2+}$ does not cause a variation of the energy of the first emission band. The value of $\tilde{\nu}_0$ of the $Ru(becbpy)_2(L\text{–}(CH_2)_n\text{–}L)^{2+}$ moiety exhibits only a small variation (15400—15600 $cm^{-1}$) with the length of the polymethylene chain.

Above 110 K the vibronic structure becomes unclear with increasing temperature and the emission maximum is shifted to lower energy (Fig. 3). When the temperature is in the range 110—160 K, the emission maximum shifts from 16500 to 15400 $cm^{-1}$ during the decay of emission (see Fig. 4). This relaxation to the final spectrum can be taken to be an indication of solvent reorganization around the reduced ligand.[38] Above 170 K, the first emission band of $[Ru(bpy)_2(L\text{–}(CH_2)_5\text{–}L)]^{2+}$ is at 15400 $cm^{-1}$ immediately after the laser excitation. Fwhm of the first emission band increases with temperature from 1450 $cm^{-1}$ at 173 K to 2180 $cm^{-1}$ at 297 K. The solvent reorganization energy involved in the formation of the lowest excited-state ($\lambda_o$) can be derived from the magnitude of fwhm through the use of Eq. 4:[39]

$$\lambda_o = \frac{(2\Delta\tilde{\nu}_{1/2})^2}{(16\ln 2)k_BT} \quad (4)$$

The average value of $\lambda_o$ is estimated to be 1980 $cm^{-1}$ in the temperature range of 170—300 K, which is much larger than that (1160 $cm^{-1}$) estimated from the emission at 77—110 K (see Table 2).[40]

The emission spectrum of $[Ru(bpy)_2(L\text{–}(CH_2)_n\text{–}L)Ru(becbpy)_2]^{4+}$ changes with time even at 77 K, as Fig. 4 shows. The emission spectra that are observed at a later time are the same as those of $[Ru(becbpy)_2(L\text{–}(CH_2)_n\text{–}L)]^{2+}$, showing that intramolecular energy transfer occurs from a donor moiety of $[Ru(bpy)_2(L\text{–}(CH_2)_n\text{–}L)]^{2+}$ to an acceptor moiety of $[Ru(becbpy)_2(L\text{–}(CH_2)_n\text{–}L)]^{2+}$.

**2. Decay of Emission.** Most of the emissions decay via a single exponential mode across a wide temperature range (77—330 K). The emission decay rates ($k_D$) of the donor moiety, $[Ru(bpy)_2(L\text{–}(CH_2)_n\text{–}L)^{2+}]$ and $[Ru(bpy)_2(bpbimH_2)]^{2+}$, (1.6—$2.4\times10^5$ $s^{-1}$ at 77 K) are varied neither by the kinds of bridging ligands nor by the coordination of the bridging ligand to another Ru(II) center, as Table 3

Table 2. The Full Width at Half Maximum (fwhm) of the First Emission Band and the Solvent Reorganization Energy of Emission of $[Ru(bpy)_2(L\text{–}(CH_2)_5\text{–}L)]^{2+}$ in Butyronitrile at Various Temperatures

| Temperature/K | fwhm/$cm^{-1}$ a) | $\lambda_o$/$cm^{-1}$ b) |
|---|---|---|
| 77 | 830 | 1160 |
| 92 | 910 | 1160 |
| 173 | 1450 | 1940 |
| 211 | 1770 | 1920 |
| 297 | 2180 | 2070 |

a) Obtained as $2\times\tilde{\nu}_{1/2}$, where $\tilde{\nu}_{1/2}$ is the half width at half-maximum on the higher energy side. b) Estimated from $(2\times\tilde{\nu}_{1/2})^2/\{16(\ln 2)k_BT\}$.

Table 1. Emission Maxima of the Donor Moieties and the Acceptor Moieties ($\tilde{\nu}_o$) and the Difference between the Donor and the Acceptor Moieties ($\Delta\tilde{\nu}_{DA}$) in Butyronitrile at 77 K Excited at 450 nm

| Compounds | $\tilde{\nu}_o/10^3$ $cm^{-1}$ | | $\Delta\tilde{\nu}_{DA}/10^3$ $cm^{-1}$ |
|---|---|---|---|
| | Donor | Acceptor | |
| $[Ru(bpy)_2(L\text{–}(CH_2)_2\text{–}L)]^{2+}$ | 16.5 (16.4[a,b]) | | |
| $[Ru(bpy)_2(L\text{–}(CH_2)_5\text{–}L)]^{2+}$ | 16.5 | | |
| $[Ru(bpy)_2(L\text{–}(CH_2)_{10}\text{–}L)]^{2+}$ | 16.5 | | |
| $[Ru(bpy)_2(bpbimH_2)Ru(bpy)_2]^{4+}$ | 16.4[b] | | |
| $[Ru(becbpy)_2(L\text{–}(CH_2)_5\text{–}L)]^{2+}$ | | 15.4 | 1.2 |
| $[Ru(bpy)_2(L\text{–}(CH_2)_2\text{–}L)Ru(becbpy)_2]^{4+}$ | | 15.5 | 1.1 |
| $[Ru(bpy)_2(L\text{–}(CH_2)_3\text{–}L)Ru(becbpy)_2]^{4+}$ | | 15.5 | 1.1 |
| $[Ru(bpy)_2(L\text{–}(CH_2)_4\text{–}L)Ru(becbpy)_2]^{4+}$ | | 15.5 | 1.0 |
| $[Ru(bpy)_2(L\text{–}(CH_2)_5\text{–}L)Ru(becbpy)_2]^{4+}$ | | 15.4 | 1.2 |
| $[Ru(bpy)_2(L\text{–}(CH_2)_6\text{–}L)Ru(becbpy)_2]^{4+}$ | | 15.4 | 1.1 |
| $[Ru(bpy)_2(L\text{–}(CH_2)_{10}\text{–}L)Ru(becbpy)_2]^{4+}$ | | 15.4 | 1.1 |
| $[Ru(bpy)_2(L\text{–}Xy\text{–}L)Ru(becbpy)_2]^{4+}$ | | 15.6 | 0.9 |
| $[Ru(bpy)_2(bpbimH_2)Ru(becbpy)_2]^{4+}$ | | 15.4 | 1.0 |

a) $[Ru(bpy)_2(L\text{–}(CH_2)_2\text{–}L)Ru(bpy)_2]^{4+}$. b) From Ref. 35 in 1 : 4 methanol–ethanol.

Table 3. Decay Rate Constants of Emission of $[Ru(bpy)_2(L–(CH_2)_n–L)]^{2+}$, $[Ru(bpy)_2(L–Xy–L)]^{2+}$, and $[Ru(bpy)_2(bpbimH_2)]^{2+}$ Moieties

| Compounds | $k_D/10^6$ s$^{-1}$ | | | | $k_{DA}/10^6$ s$^{-1}$ | | |
|---|---|---|---|---|---|---|---|
| | 77 K[a] | 170 K[b] | 298 K[b] | | 77 K[c] | 170 K[d] | 298 K[d] |
| $[Ru(bpy)_2(L–(CH_2)_2–L)]^{2+}$ | 0.16 (0.24[e]) | 0.58 | 1.67 | $[Ru(bpy)_2(L–(CH_2)_2–L)Ru(becbpy)_2]^{4+}$ | 7.6(25[f]) | 8.6 | 33.0 |
| $[Ru(bpy)_2(L–(CH_2)_3–L)]^{2+}$ | 0.24(0.25[e]) | | 1.44 | $[Ru(bpy)_2(L–(CH_2)_3–L)Ru(becbpy)_2]^{4+}$ | 6.2(26[f]) | 6.1 | 32.5 |
| $[Ru(bpy)_2(L–(CH_2)_4–L)]^{2+}$ | 0.22(0.24[e]) | | 1.59 | $[Ru(bpy)_2(L–(CH_2)_4–L)Ru(becbpy)_2]^{4+}$ | 3.7(12[f]) | | 18.9 |
| $[Ru(bpy)_2(L–(CH_2)_5–L)]^{2+}$ | 0.21(0.23[e]) | 0.71 | 1.50 | $[Ru(bpy)_2(L–(CH_2)_5–L)Ru(becbpy)_2]^{4+}$ | 3.1(12[f]) | 3.0 | 14.5 |
| $[Ru(bpy)_2(L–(CH_2)_6–L)]^{2+}$ | 0.23 | | 1.50 | $[Ru(bpy)_2(L–(CH_2)_6–L)Ru(becbpy)_2]^{4+}$ | 2.0(7[f]) | | 18.0 |
| $[Ru(bpy)_2(L–(CH_2)_{10}–L)]^{2+}$ | 0.22 | 0.72 | 1.47 | $[Ru(bpy)_2(L–(CH_2)_{10}–L)Ru(becbpy)_2]^{4+}$ | 0.68(1.6[f]) | 1.1 | 4.3 |
| $[Ru(bpy)_2(L–Xy–L)]^{2+}$ | 0.23 | | 1.48 | $[Ru(bpy)_2(L–Xy–L)Ru(becbpy)_2]^{4+}$ | 3.2(8[f]) | 2.3 | 14.3 |
| $[Ru(bpy)_2(bpbimH_2)]^{2+}$ | 0.24 | 0.88 | 1.85 (1[g]) | $[Ru(bpy)_2(bpbimH_2)Ru(becbpy)_2]^{4+}$ | 55 | 41 | 142 |

a) Emission decay rate constant of donor moieties monitored at 16500 cm$^{-1}$. b) Emission decay rate constant of donor moieties monitored at 15400 cm$^{-1}$. c) Emission decay rate constant of donor moieties in the dinuclear compounds monitored at 16500 cm$^{-1}$. d) Emission decay rate constant of donor moieties in the dinuclear compounds monitored at 15400 cm$^{-1}$. e) Emission decay rate constant of $[Ru(bpy)_2(L–(CH_2)_n–L)Ru(bpy)_2]^{4+}$ monitored at 16500 cm$^{-1}$. f) Emission rate constant of the minor and fast decaying component. g) Emission decay rate constant of $[Ru(bpy)_2(bpbimH_2)Ru(bpy)_2]^{4+}$ monitored at 16400 cm$^{-1}$.

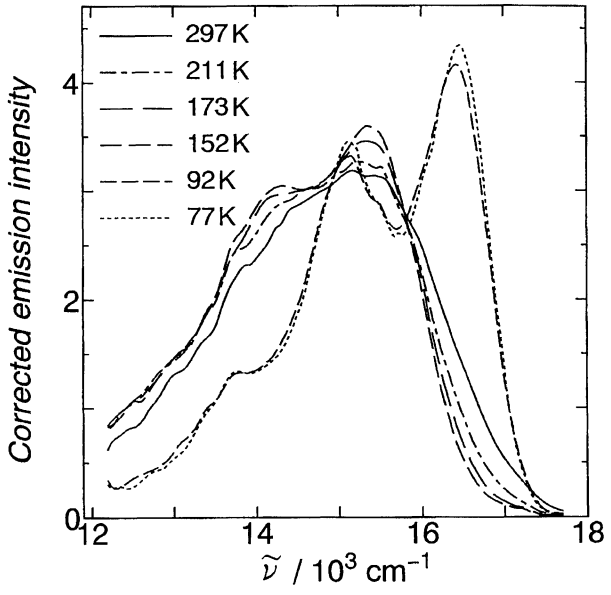


Fig. 3. Emission spectrum of $[Ru(bpy)_2(L–(CH_2)_5–L)]^{2+}$ with the excitation at 450 nm in butyronitrile at various temperatures.

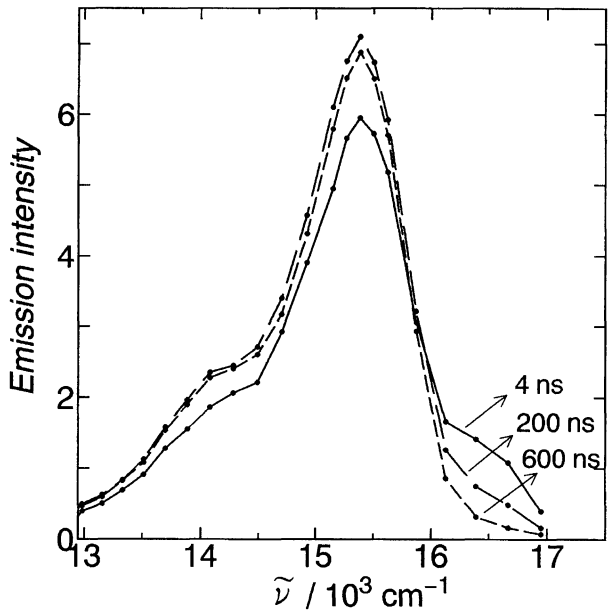


Fig. 4. Time-resolved emission spectra of $[Ru(bpy)_2(L–(CH_2)_5–L)Ru(becbpy)_2]^{2+}$ in butyronitrile at 77 K at 4, 200, and 600 ns after the laser pulse.

shows. A small difference in $k_D$ between the mononuclear and the symmetrical dinuclear compounds was observed only for the shortest bridging ligand ($n$=2). The emission decay of the Ru(becbpy)$_2^{2+}$ moiety ($1.9—2.1\times10^5$ s$^{-1}$ at 77 K) is insensitive to the nature of the bridging ligands. The decay rates of the emissions gradually increased with temperature up to 280 K, and then more dramatically above 280 K, as shown in Fig. 5.

As for the unsymmetrical dinuclear compound, $[(bpy)_2Ru(L–(CH_2)_5–L)Ru(becbpy)_2]^{4+}$, the emission of the $[Ru(bpy)_2]^{2+}$ moiety monitored at 16500 cm$^{-1}$ decays rapidly with a rate constant ($k_{DA}$). The emission of the $[Ru(becbpy)_2(L–(CH_2)_5–L)]^{2+}$ moiety at 15200 cm$^{-1}$ is observed to increase during the emission decay of the $[Ru(bpy)_2(L–(CH_2)_5–L)]^{2+}$ moiety. The emission from the $[Ru(bpy)_2(L–(CH_2)_5–L)]^{2+}$ moiety at 77 K decays in a biexponential mode; the major component ($f$=0.8) decays with $k_{DA}=3.1\times10^6$ s$^{-1}$ and the minor one ($f$=0.2) with $k_{DA}=12\times10^6$ s$^{-1}$. The minor decay component can be ascribed to the presence of a folded conformer of the polymethylene chain with a shorter Ru(II)–Ru(II) distance than the extended conformer has. The magnitude of $k_{DA}$ is larger than that of $[Ru(bpy)_2(L–SP–L)]^{2+}$ ($k_D$) at any temperature, and is weakly dependent on temperature, as shown in Fig. 5.

## Discussion

**Distance Dependence of Excitation Energy Transfer.** The excited MLCT state of the donor moiety, Ru(bpy)$_2^{2+}$, in the unsymmetrical diruthenium(II) compounds decays via three channels: excitation energy transfer to $[Ru(becbpy)_2(L–(CH_2)_n–L)]^{2+}$ with a rate constant $k_{EN}$, emis-

sion of phosphorescence ($k_p$), and nonradiative transition to the ground state ($k_{non}$). Since the decay rates of the donor moiety, $k_D$, are not affected by the coordination to another $Ru(bpy)_2^{2+}$ moiety, the coordination of $Ru(becbpy)_2^{2+}$ moiety to $[Ru(bpy)_2(L\text{–}(CH_2)_n\text{–}L)]^{2+}$ does not affect the sum of $k_{non}$ and $k_p$ of the donor moiety. Consequently, the difference between $k_D$ and $k_{DA}$ is taken as the value of $k_{EN}$. As for the dinuclear compounds with the shortest bridging ligands, $[Ru(bpy)_2(bpbimH_2)Ru(becbpy)_2]^{4+}$ and $[Ru(bpy)_2(L\text{–}(CH_2)_2\text{–}L)Ru(becbpy)_2]^{4+}$, the value of $k_{DA}$ can be regarded as that of $k_{EN}$ because the values of $k_{DA}$ ($55\times10^6$ $s^{-1}$ and $7.6\times10^6$ $s^{-1}$ at 77 K, respectively) are much larger than those of $k_D$ ($0.24\times10^6$ $s^{-1}$ and $0.16\times10^6$ $s^{-1}$ at 77 K). The magnitude of $k_{EN}$ at 77 K, which varies from $0.4\times10^6$ $s^{-1}$ for $[Ru(bpy)_2(L\text{–}(CH_2)_{10}\text{–}L)Ru(becbpy)_2]^{4+}$ to $7.4\times10^6$ $s^{-1}$ for $[Ru(bpy)_2(L\text{–}(CH_2)_2\text{–}L)Ru(becbpy)_2]^{4+}$, are weakly dependent on the distance between the Ru(II) centers, as shown in Table 4.

The weak dependence of $k_{EN}$ on the $Ru^{2+}$–$Ru^{2+}$ distance ($r$) is well explained by the Förster mechanism (Eq. 3). As Fig. 6 shows, $\log k_{EN}$ is linearly correlated with $\log(1/r^6)$, where the distance between the Ru(II) cations is taken, to the first approximation, as the dipole–dipole distance. An extended form of the polymethylene chain is assumed to be dominant for $[Ru(bpy)_2(L\text{–}(CH_2)_n\text{–}L)Ru(becbpy)_2]^{4+}$, inasmuch as the electrostatic repulsion between the Ru(II) centers is the weakest for the extended conformer. Because the increasing length of the polymethylene chain reduces

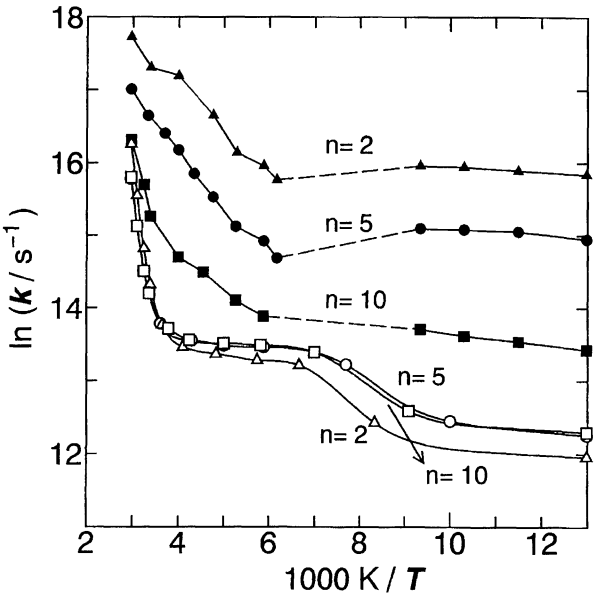


Fig. 5. Temperature dependence of the emission decay ($k_D$ and $k_{AD}$) of the $[Ru(bpy)_2(L\text{–}(CH_2)_5\text{–}L)]^{2+}$ moiety at 77—330 K. △, ○, □: $k_D$ for $[Ru(bpy)_2(L\text{–}(CH_2)_n\text{–}L)]^{2+}$ ($n$=2, 5, and 10); ▲, ●, ■: $k_{DA}$ for $[Ru(bpy)_2(L\text{–}(CH_2)_n\text{–}L)Ru(becbpy)_2]^{4+}$ ($n$=2, 5, and 10).

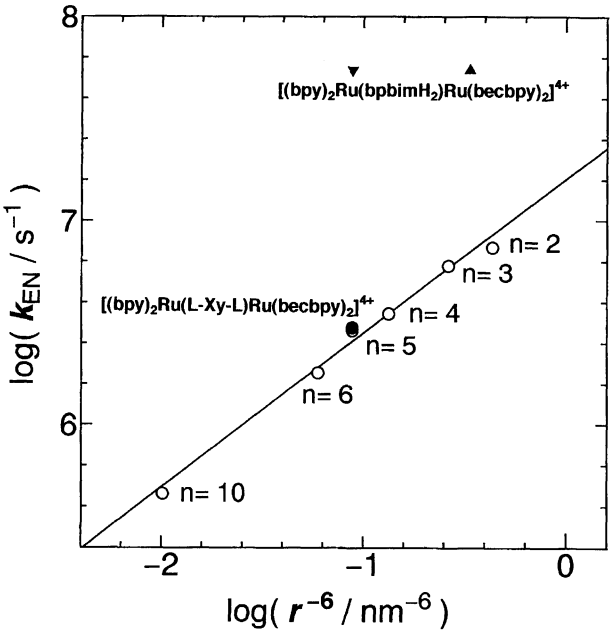


Fig. 6. Plot of $\log k_{EN}$ vs. $\log(1/r^6)$, where the energy transfer rate ($k_{EN}$) and the $Ru^{2+}$–$Ru^{2+}$ distance ($r$) are taken as difference between $k_{DA}$ and $k_D$ and the dipole–dipole distance, respectively. The magnitude of the rate constants are measured in butyronitrile at 77 K. ○: $[Ru(bpy)_2(L\text{–}(CH_2)_n\text{–}L)Ru(becbpy)_2]^{4+}$; ●: $[Ru(bpy)_2(L\text{–}Xy\text{–}L)Ru(becbpy)_2]^{4+}$; ▲ and ▼: the long size and the short size isomers of $[(bpy)_2Ru(bpbimH_2)Ru(becbpy)_2]^{4+}$, respectively.[45]

Table 4. Rates of the Energy Transfer ($k_{EN}$ and $k_{EN}^{cal}$) Observed and Calculated, Respectively

| Compounds | $k_{EN}/10^6$ $s^{-1}$ | | | $E_a/cm^{-1}$ a) | $r$/nm b) | $k_{EN}^{cal}/10^6$ $s^{-1}$ | a.e.c. c) | | |
|---|---|---|---|---|---|---|---|---|---|
| | 77 K | 170 K | 298 K | | | 77 K | 77 K | 170 K | 298 K |
| $[Ru(bpy)_2(L\text{–}(CH_2)_2\text{–}L)Ru(becbpy)_2]^{4+}$ | 7.4 | 8 | 33 | 23 (400 d)) | 1.15 | 22 | – | – | – |
| $[Ru(bpy)_2(L\text{–}(CH_2)_3\text{–}L)Ru(becbpy)_2]^{4+}$ | 6.0 | 5.3 | 31 | – (510 d)) | 1.25 | 12 | – | – | – |
| $[Ru(bpy)_2(L\text{–}(CH_2)_4\text{–}L)Ru(becbpy)_2]^{4+}$ | 3.5 | 2.3 | 17 | – | 1.4 | 6.1 | – | – | – |
| $[Ru(bpy)_2(L\text{–}(CH_2)_5\text{–}L)Ru(becbpy)_2]^{4+}$ | 2.9 | 2.3 | 13 | 24 (520 d)) | 1.5 | 4.0 | 5.5 | 1.7 | 2.6 |
| $[Ru(bpy)_2(L\text{–}(CH_2)_6\text{–}L)Ru(becbpy)_2]^{4+}$ | 1.8 | – | – | – | 1.6 | 2.7 | – | – | – |
| $[Ru(bpy)_2(L\text{–}(CH_2)_{10}\text{–}L)Ru(becbpy)_2]^{4+}$ | 0.46 | 0.35 | 3 | 57 (630 d)) | 2.15 | 0.46 | – | – | – |
| $[Ru(bpy)_2(L\text{–}Xy\text{–}L)Ru(becbpy)_2]^{4+}$ | 3.0 | 1.8 | 14 | – (560 d)) | 1.5 | 4.0 | – | – | – |
| $[Ru(bpy)_2(bpbimH_2)Ru(becbpy)_2]^{4+}$ | 55 | 40 | 140 | 42 (350 d)) | 1.5 e) | 4.0 e) | 1.28 f) | 0.42 f) | 0.72 f) |

a) Activation energy of energy transfer in a region of 77—110 K. b) A distance between ruthenium(II) centers is calculated by assuming the bond lengths, $r_{C-C}$=0.154, $r_{C-N}$=0.13, and $r_{Ru-N}$=0.21 nm. c) Absorption–emission coupling integral in $10^{-15}$ $cm^3$ $dm^3$ $mol^{-1}$ (see Eq. 3). d) Activation energy of energy transfer in a region of 170—330 K. e) See Ref. 45. f) Absorption–emission overlap integral in $10^{-4}$ cm (see Eq. 2).

the electrostatic repulsion between the cationic centers, the fraction of the conformer that is extended might be expected to decrease for the longer chain compounds. The observed slope of 0.76 for the plot of log $k_{EN}$ vs. log $(1/r^6)$ (see Fig. 6), which is a little smaller than unity, implies that the average distance between the transition dipoles of the longer chain compounds is less than that of the extended conformer of the polymethylene chain, even at 77 K. *trans*-to-*gauche* Conversion of the long polymethylene chain shortens the $Ru^{2+}$–$Ru^{2+}$ distance at higher temperatures. Meanwhile, the contribution of the exchange interaction to the energy transfer in the short chain $[Ru(bpy)_2(L–(CH_2)_2–L)Ru(becbpy)_2]^{4+}$ compound would increase the energy transfer rate and the slope of the linear relationship. Seemingly, an exchange interaction does not play a major role in the energy transfer reactions of $[Ru(bpy)_2(L–(CH_2)_n–L)Ru(becbpy)_2]^{4+}$ ($n$=2—6, and 10). The following implies no contribution of exchange interaction to the energy transfer. That is, the *p*-xylene moiety of the bridging ligand does not enhance the energy transfer rate in comparison with the pentane bridged biruthenium compound with the same $Ru^{2+}$–$Ru^{2+}$ distance.

The rates of energy transfer can be estimated by putting the following quantities into Eq. 3, based on the dipole–dipole interaction mechanism (Table 4): $1/\tau_0=8.2\times10^4$ $s^{-1}$, $\varepsilon_A=1.7\times10^3$ (77 K) and $1.4\times10^3$ (300 K) $dm^3\,mol^{-1}\,cm^{-1}$ at $17.3\times10^3$ $cm^{-1}$, $\tilde{\nu}_D^{max}=16.5\times10^3$ $cm^{-1}$, $n$=1.52 (77 K), 1.46 (170 K), and 1.38 (300 K),[44] $r$=1.15—2.15 nm,depending on the number of methylene groups. In the estimate of the absorption–emission coupling integral, the spin multiplicity should be retained between the emission and the absorption. For this purpose, the absorption–emission coupling (Eq. 3) was calculated between the lowest and weak absorption band of an acceptor and the whole emission spectrum of a donor in a region of 15800—17300 $cm^{-1}$. The energy transfer rates that are calculated ($k_{EN}^{cal}$) are in good agreement with those observed, as shown in Table 4. The extent of the absorption–emission coupling integral ($5.5\times10^{-15}$ $cm^3\,M^{-1}$ for $[Ru(bpy)_2(L–(CH_2)_5–L)Ru(becbpy)_2]^{4+}$ at 77 K) is nearly constant among the dinuclear compounds, as is expected from the nearly constant energy gap ($\Delta\tilde{\nu}_{DA}$). The slightly larger values of $k_{EN}^{cal}$ suggest that there is more mixing of the singlet state with the triplet state in absorption than in emission.

In the case of $[(bpy)_2Ru(bpbimH_2)Ru(becbpy)_2]^{4+}$, the energy transfer observed at 77 K was faster by a factor of 14 (4[45]) than that calculated by using Eq. 3 (see Table 4). This is also shown in Fig. 6 where the rate is higher than the others. It is likely that the exchange interaction is predominant for the fast energy transfer. The magnitude of absorption–emission overlap in Eq. 2 can be estimated from the intensities of absorption and emission, the former of which is normalized to the integrated one of singlet–triplet charge transfer band drawn by a thin chain line in Fig. 2. The possible largest magnitude of the matrix element ($H_{rp}$) is estimated to be 0.6 $cm^{-1}$ from the magnitude of $k_{EN}$ observed and the absorption–emission overlaps estimated.

According to Closs et al.,[1,22—24] two-electron two-center integrals for energy transfer via an exchange mechanism can be the product of the exchange integrals between HOMOs and between the LUMOs to a first-order approximation. The magnitude of the one-electron two-center exchange integral between the HOMO ($d_\pi$-orbital) of $[Ru(bpy)_2(bpbimH_2)]^{2+}$ and $[Ru(becbpy)_2]^{2+}$ is estimated to be as much as that (80 $cm^{-1}$) of $[(bpy)_2Ru(II)(bpbimH_2)Ru(III)(bpy)_2]^{5+}$.[35] The other integral between the LUMOs of both $bpbimH_2$ and becbpy is inferred to be much smaller than that between the HOMOs.

**Temperature Dependence of Energy Transfer Rates.** The temperature dependence of the energy transfer rates is rather complex, as shown in Fig. 7. The very slow rise in the rates with increasing temperature in the range 77—110 K is due to the temperature-independent absorption–emission coupling integral. The rate of energy transfer decreases with increasing temperature at 110—170 K, where the highest energy emission bands began to shift to low energy (from 16500 to 15400 $cm^{-1}$). The decrease of the absorption–emission coupling integral by one-third up to 170 K (see Table 4) causes a reduction of the rate to one-third of that estimated from the extrapolation of the slightly increasing rate with temperature in the temperature 77—110 K region (see Fig. 7).

Above 170 K, the rates of excitation energy transfer gradually increase with temperature. The apparent activation energies for the energy transfer processes at 170—330 K are the smallest (360 $cm^{-1}$) for $Ru(bpy)_2(bpbimH_2)Ru(becbpy)_2^{4+}$ and the largest (630 $cm^{-1}$) for $[Ru(bpy)_2(L–(CH_2)_{10}–L)Ru$-

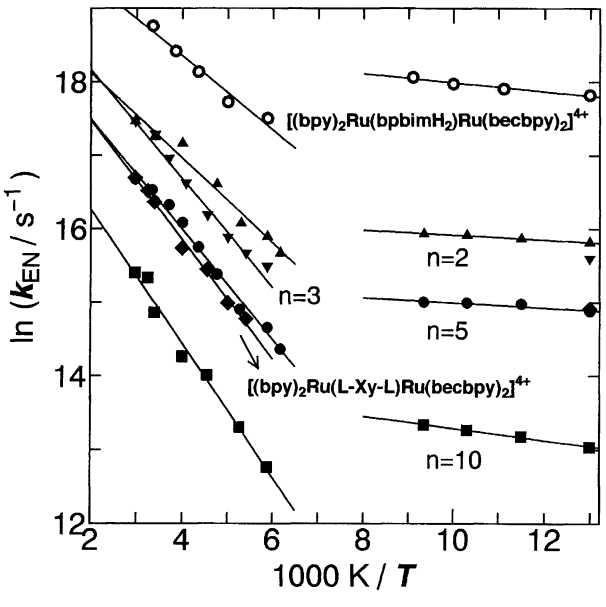


Fig. 7. Temperature dependence of the energy transfer rate, $k_{EN}$ ($=k_{DA}-k_D$), obtained by monitoring the emission decay of the donor at 16500 $cm^{-1}$. The energy donor and the energy acceptor are $Ru(bpy)_2^{2+}$ moiety and $Ru(becbpy)_2^{2+}$ moiety, respectively. ▲, ▼, ●, ■: for $[Ru(bpy)_2(L–(CH_2)_n–L)Ru(becbpy)_2]^{4+}$ ($n$=2, 3, 5, and 10); ◆: $[Ru(bpy)_2(L–Xy–L)Ru(becbpy)_2]^{4+}$; ○: $[(bpy)_2Ru(bpbimH_2)Ru(becbpy)_2]^{4+}$.

$(becbpy)_2]^{4+}$. A part of the increase in the energy transfer rate with increasing temperature can be accounted for in terms of either FCWD or the absorption–emission coupling. The donor emission exhibits more overlap with the acceptor absorption in the region 16000—17500 $cm^{-1}$ as the fwhm of the first emission band increases from 1450 to 2180 $cm^{-1}$ with temperature above 170 K. Both the FCWD and the absorption–emission coupling integrals (Eqs. 2 and 3) between the emission and the absorption increase by 60% from 170 to 297 K (see Table 4). However, the increase of the integrals with temperature can account for only 25 and 43% of the activation energy for energy transfer within $[Ru(bpy)_2(L–(CH_2)_5–L)Ru(becbpy)_2]^{4+}$ and $[Ru(bpy)_2(bpbimH_2)Ru(becbpy)_2]^{4+}$, respectively. The rest of the activation energy can be attributed to the effect of temperature on the dipole–dipole distance for the dinuclear compound with a polymethylene chain of $n \geq 3$. A rise in temperature allows the folding of the polymethylene chain or the libration of the flexible polymethylene chain. A shorter distance due to both the folded conformer and the libration of a polymethylene chain at higher temperatures would give rise to more dipole–dipole interaction (faster rate) in comparison with the extended conformer.

**Concluding Remarks.** Excitation energy transfer from the $Ru(bpy)_2^{2+}$ moiety to the $Ru(becbpy)_2^{2+}$ moiety within ligand bridged diruthenium(II) compounds occurred with the rate constant of $k_{EN}$ observed. The energy transfer within $[Ru(bpy)_2(L–(CH_2)_n–L)Ru(becbpy)_2]^{2+}$ with the Ru–Ru distance ($r$) at 77 K is ascribed to the dipole–dipole interaction. The log $k_{EN}$ plot against log $(1/r^6)$ is linearly correlated with a slope of 0.76, implying that the average distance between the transition dipoles of the longer chain compounds is less than that of the extended conformer of the polymethylene chain. The weak temperature dependence of the energy transfer rate in the region of 77—110 K is explained in terms of the absorption–emission coupling integral. The rise in temperature above 170 K makes the coupling integral greater and probably makes the Ru–Ru distance shorter. The fast energy transfer within $[(bpy)_2Ru(bpbimH_2)Ru(becbpy)_2]^{4+}$ is ascribed to the substantial exchange interaction between the donor and acceptor moieties.

We are grateful to Professor Morton Z. Hoffman (Boston University) for many helpful comments. We thank Dr. Takashi Komorita for providing us with computer programs for the analysis of the absorption spectra. The present work was supported by a Grant-in-Aid for Scientific Research Nos. 06640655, 05740361, and 06640722 to A. Y., K. N., and N. I. and a Grant-in-Aid on Priority-Area-Research "Photoreaction Dynamics" No. 06239101 to T.O. from the Ministry of Education, Science, Sports and Culture.

## References

1) G. L. Closs, L. T. Calcaterra, N. J. Green, K. W. Penfield, and J. R. Miller, *J. Phys. Chem.*, **90**, 3673 (1986).
2) P. Chen, R. Duesing, D. K. Graff, and T. J. Meyer, *J. Phys. Chem.*, **95**, 5850 (1991).
3) D. B. MacQueen and K. S. Schanze, *J. Am. Chem. Soc.*, **113**, 7470 (1991).
4) P. Finckh, H. Heitele, M. Volk, and M. E. Michel-Beyele, *J. Phys. Chem.*, **92**, 6584 (1988).
5) N. Liag, J. R. Miller, and G. L. Closs, *J. Am. Chem. Soc.*, **112**, 5353 (1990).
6) K. Nozaki, T. Ohno, and M. Haga, *J. Phys. Chem.*, **96**, 10880 (1992).
7) A. Yoshimura, K. Nozaki, N. Ikeda, and T. Ohno, *J. Am. Chem. Soc.*, **115**, 7521 (1993).
8) M. J. Weaver, *Chem. Rev.*, **92**, 463 (1992).
9) J. D. Simon, *Acc. Chem. Res.*, **21**, 128 (1988).
10) K. Tominaga, D. A. V. Kliner, A. E. Johnson, N. E. Levinger, and P. F. Barbara, *J. Chem. Phys.*, **98**, 1228 (1993).
11) H. Oevering, M. N. Paddon-Row, M. Heppener, A. M. Oliver, E. Cotsaris, J. W. Verhoeven, and N. S. Hush, *J. Am. Chem. Soc.*, **109**, 3258 (1984).
12) P. Siddarth and R. A. Marcus, *J. Phys. Chem.*, **94**, 2985 (1990).
13) S. Franzen, R. F. Goldstein, and S. G. Boxer, *J. Phys. Chem.*, **97**, 3040 (1993).
14) M. Newton, *Chem. Rev.*, **91**, 767 (1991).
15) J. Jortner, *J. Chem. Phys.*, **64**, 4860 (1976).
16) D. L. Dexter, *J. Chem. Phys.*, **21**, 836 (1953).
17) G. Basu, M. Kubasik, D. Anglos, and A. Kuki, *J. Phys. Chem.*, **97**, 3956 (1993).
18) T. Förster, *Ann. Phys. (Leipzig)*, **2**, 55 (1948).
19) Z. Murtaza, A. D. Zipp, L. A. Worl, D. Graff, W. E. Jones, Jr., W. D. Betes, and T. J. Meyer, *J. Am. Chem. Soc.*, **113**, 5113 (1991).
20) D. B. MacQueen, J. R. Eyler, and K. S. Schanze, *J. Am. Chem. Soc.*, **114**, 1897 (1992).
21) R. Tamilarasan and J. F. Endicott, *J. Phys. Chem*, **90**, 1027 (1986).
22) M. E. Sigman and G. L. Closs, *J. Phys. Chem.*, **95**, 5012 (1991).
23) G. L. Closs, P. Piotrowiak, J. M. MacInnis, and G. R. Fleming, *J. Am. Chem. Soc.*, **110**, 2652 (1988).
24) G. L. Closs, M. D. Johnson, J. R. Miller, and P. Piotrowiak, *J. Am. Chem. Soc.*, **111**, 3751 (1989).
25) H. Katayama, S. Ito, and M. Yamamoto, *J. Phys. Chem.*, **95**, 3480 (1991).
26) R. H. Schmehl, R. A. Auerbach, and W. F. Wacholz, *J. Phys. Chem.*, **92**, 6202 (1988).
27) C. K. Rhu and R. H. Schmehl, *J. Phys. Chem.*, **93**, 7691 (1988).
28) M. Furue, K. Maruyama, Y. Kanematsu, T. Kushida, and M. Kamachi, *Coord. Chem. Rev.*, **132**, 201 (1994).
29) C. A. Bignozzi, M. T. Indelli, and F. Scandola, *J. Am. Chem. Soc.*, **111**, 5192 (1989).
30) S. Boyde, G. F. Stouse, W. E. Jones, and T. J. Meyer, *J. Am. Chem. Soc.*, **111**, 7448 (1989).
31) Y. Lei, T. Buronda, and J. F. Endicott, *J. Am. Chem. Soc.*, **112**, 8820 (1990).
32) Y. Wang and K. S. Schanze, *Inorg. Chem.*, **33**, 1354 (1994).
33) K. Nozaki and T. Ohno, *Coord. Chem. Rev.*, **132**, 215 (1994).
34) H. T. S. Britton and R. A. Robinson, *J. Chem. Soc.*, **458**, 1456 (1931).
35) T. Ohno, K. Nozaki, and M. Haga, *Inorg. Chem.*, **31**, 548 (1992).
36) M. Haga, T. Ano, T. Ishizaki, K. Kano, K. Nozaki, and T.

Ohno, *J. Chem. Soc., Dalton Trans.*, **1994**, 263.

37) W. F. Wacholtz, R. A. Auerbach, and R. H. Schmehl, *Inorg. Chem.*, **25**, 227 (1986).

38) J. Ferguson, E. R. Krausz, and M. Maeder, *J. Phys. Chem.*, **89**, 1852 (1985).

39) R. A. Marcus, *J. Phys. Chem.*, **93**, 3078 (1989).

40) The variation of $\lambda_o$ with temperature may be an artifact, since the spectral analysis is oversimplified in comparison with the procedures used in previous works.[41,42] However, this procedure gives rise to the temperature-independent value of $\lambda_o$ (375 $cm^{-1}$) in crystalline $[Ru(bpy)_3](PF_6)_2$.[43]

41) J. V. Casper, T. D. Westmoreland, G. H. Allen, P. G. Bradley, T. J. Meyer, and W. H. Woodruff, *J. Am. Chem. Soc.*, **106**, 3492 (1984).

42) R. S. Lumpkin and T. J. Meyer, *J. Phys. Chem.*, **90**, 5307 (1986).

43) N. Ikeda, A. Islam, and T. Ohno, to be published.

44) J. A. Riddick, W. B. Bunger, and T. K. Sakano, "Organic Solvents," 4th ed, Wiley-Interscience, New York (1986), p. 587.

45) The bridging ligand of $bpbimH_2$ contains two isomers.[6] The distance between the ruthenium(II) centers linked by the shorter-size isomer is 1.2 nm, for which the energy transfer rate is calculated to be $15\times10^6$ $s^{-1}$.